Conventional superconductivity in $SrPd_2Ge_2$

T. K. Kim,[1,2,*] A. N. Yaresko,[3] V. B. Zabolotnyy,[2] A. A. Kordyuk,[2,4] D. V. Evtushinsky,[2] N. H. Sung,[5] B. K. Cho,[5,6] T. Samuely,[7] P. Szabó,[8] J. G. Rodrigo,[9] J. T. Park,[3] D. S. Inosov,[3] P. Samuely,[8] B. Büchner,[2] and S. V. Borisenko[2]

[1]*Diamond Light Source Ltd., Didcot OX11 0DE, United Kingdom*

[2]*Leibniz-Institute for Solid State and Materials Research Dresden, P.O.Box 270116, D-01171 Dresden, Germany*

[3]*Max Planck Institute for Solid State Research, Heisenbergstraβe 1, D-70569 Stuttgart, Germany*

[4]*Institute of Metal Physics, National Academy of Sciences of Ukraine, 03142 Kyiv, Ukraine*

[5]*School of Materials Science and Engineering, Gwangju Institute of Science and Technology, Gwangju 500-712, Korea*

[6]*Department of Nanobio Materials and Electronics, Gwangju Institute of Science and Technology, Gwangju 500-712, Korea*

[7]*Institute of Physics, Faculty of Science, P. J. Šafárik University, Park Angelinum 9, SK-04001 Košice, Slovakia*

[8]*Centre of Low Temperature Physics, Institute of Experimental Physics, Slovak Academy of Sciences, Watsonova 47, SK-04001 Košice, Slovakia*

[9]*Laboratorio de Bajas Temperaturas, Departamento de Física de la Materia Condensada, Instituto de Ciencia de Materiales Nicolás Cabrera, Universidad Autónoma de Madrid, E-28049 Madrid, Spain*

(Received 2 June 2011; revised manuscript received 22 November 2011; published 25 January 2012)

The electronic structure of $SrPd_2Ge_2$ single crystals is studied by angle-resolved photoemission spectroscopy (ARPES), scanning tunneling spectroscopy (STS), and band structure calculations within the local-density approximation (LDA). The STS measurements show a single s-wave superconducting energy gap $\Delta(0) = 0.5$ meV. The photon-energy dependence of the observed Fermi surface reveals a strongly three-dimensional character of the corresponding electronic bands. By comparing the experimentally measured and calculated Fermi velocities a renormalization factor of 0.95 is obtained, which is much smaller than typical values reported in Fe-based superconductors. We ascribe such an unusually low band renormalization to the different orbital character of the conduction electrons and, using ARPES and STS data, argue that $SrPd_2Ge_2$ is likely to be a conventional superconductor, which makes it clearly distinct from isostructural iron pnictide superconductors of the "122" family.

DOI: 10.1103/PhysRevB.85.014520 PACS number(s): 74.25.Jb, 74.70.Xa, 71.18.+y, 71.20.−b

I. INTRODUCTION

Since the discovery of superconductivity in iron pnictides,[1] several families of these novel superconductors have been studied. Among them, a broad family of the so-called "122" superconductors based on AFe_2As_2 systems (A = Ca, Sr, or Ba) with transition temperatures up to $T_c \approx 38$ K was prepared by a charge-carrier doping, i.e., by partial substitution of alkaline metals for alkaline-earth metals or by partial replacement of Fe (in $[Fe_2As_2]$ layers) with other $3d$ transition metals, such as Co or Ni,[2,3] or by partial substitution of As with P.[4,5] Similar to the superconducting cuprates,[6] all these compounds have quasi-two-dimensional crystal structures formed by iron-pnictide layers separated by different buffer layers. The partially occupied bands from these iron-pnictide layers determine the electronic structure of the materials in the near-Fermi-level (FL) region, which in turn determines the superconducting properties.

One of the puzzles of iron-based superconductors is the role of magnetism and the effects of chemical and structural tuning on superconducting properties. Thus, the recent discovery[7] of a new low-temperature ($T_c \approx 2.7$ K) stoichiometric superconductor $SrPd_2Ge_2$ isostructural with the group of 122 iron pnictides appears intriguing not only because this compound is pnictogen and chalcogen free but also because it has the magnetic metal (Fe) completely replaced by the nonmagnetic metal (Pd). It is, therefore, interesting whether $SrPd_2Ge_2$ starts a new family of exotic superconductors similar to pnictides. In this paper we show that $SrPd_2Ge_2$ is, in fact, very different from the 122 family of pnictides: its electronic structure is strongly three-dimensional (3D) and is well described within local-density approximation (LDA), and it has a single isotropic superconducting gap with $2\Delta/kT_c = 4$, not largely exceeding the Bardeen-Cooper-Schrieffer (BCS) theory universal value, thus leaving no space for exotic electronic states.

II. METHODS

Single crystals of $SrPd_2Ge_2$ of $\sim 1 \times 2$ mm^2 size were grown by the high-temperature-flux method using PdGe self-flux as described in Ref. 8.

Temperature- and field-dependent magnetizations of single crystals were measured by a Quantum Design superconducting quantum interference device (SQUID) magnetometer. Zero-field cooling (ZFC) magnetization was measured with increasing temperature in a field $H = 10$ Oe along the ab plane of the sample after cooling down to 2 K in zero field, and the field-cooling (FC) magnetization was measured with increasing temperature in the same field. For a single crystal with a mass of 4 mg the superconducting transition temperature was found to be $T_c \approx 2.7$ K (Fig. 1).

Scanning tunneling spectroscopy (STS) measurements were done using a homemade low-temperature scanning tunneling microscope (STM) head developed in Košice in collaboration with Universidad Autónoma de Madrid[9] and installed in a commercial Janis SSV cryomagnetic system with a ^{3}He refrigerator and controlled by Nanotec's Dulcinea SPM electronics. An atomic-size, sharp superconducting tip made of pure lead was scanned over the $SrPd_2Ge_2$ sample with bias voltage applied to the tip, while the sample was grounded.

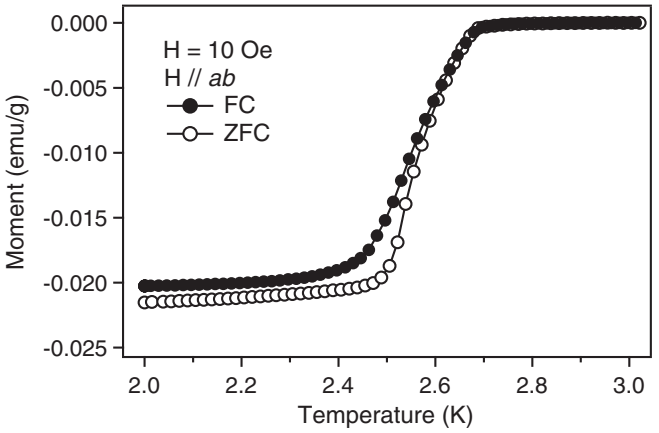

FIG. 1. Temperature dependence of magnetization of the $SrPd_2Ge_2$ single crystal with a field of 10 Oe, perpendicular to the c axis, in both field-cooling (FC) and zero-field-cooling (ZFC) modes.

Photoemission experiments were performed at the 1^3 ARPES setup at BESSY based on the R4000 Scienta electron-energy analyzer.[10] The geometry of the experiments included a fixed analyzer and a sample mounted on a ^{3}He cryomanipulator that enables rotation about the vertical axis. The entrance slit of the analyzer was vertically aligned, and the angle between the optical axis of the analyzer lenses and the incident synchrotron beam was ~45°. All spectra have been measured with linear horizontal polarization. Single-crystalline samples were cleaved *in situ* in ultrahigh vacuum at 35 K. The measurements were performed at temperatures around 1 K, and the overall energy and angular resolutions were set to 10 meV and 0.2°, respectively.

Electronic band structure calculations were performed for the experimental crystal structure of $SrPd_2Ge_2$ from Ref. 7 within the LDA using the linear muffin-tin orbital (LMTO) method.[11,12]

III. RESULTS AND DISCUSSION

The crystal structure of $SrPd_2Ge_2$ is the same as in $BaFe_2As_2$, but its electronic structure is expected to exhibit a much stronger 3D character.[13]

Our LDA calculations show that, in contrast to the isostructural iron pnictides, in which Fe d states responsible for very peculiar nesting of electron and holelike sheets of the Fermi surface are partially occupied, the Pd d states in $SrPd_2Ge_2$ are completely filled, and bands crossing the Fermi level are formed by delocalized Ge p and Sr d states with only a minor admixture of the Pd d states (see Fig. 2). As a result, the calculated Fermi surface (FS) shown in Fig. 3 reveals a 3D character of the $SrPd_2Ge_2$ electronic structure with a very strong k_z dependence of the conduction bands. The calculated two-dimensional Fermi surfaces corresponding to the cuts of the Brillouin zone (BZ) with different k_z values are shown in Figs. 3(b)–3(d).

Aiming to examine the topology of the Fermi surface of $SrPd_2Ge_2$ experimentally, an angle-resolved photoemission spectroscopy (ARPES) study has been performed over an extended area in momentum space. The momentum distribution maps (MDMs) derived from the ARPES experiment with

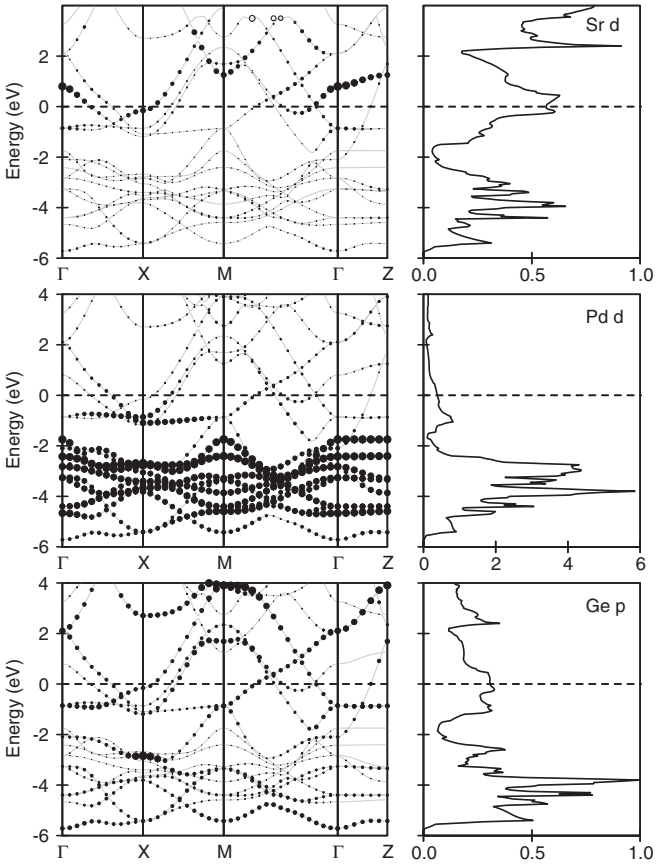

FIG. 2. LDA band structure and density of states for $SrPd_2Ge_2$. Bands in different panels (from top to bottom) are marked with circles, whose radii are proportional to the weight of Sr d, Pd d, and Ge p states in the corresponding Bloch wave functions.

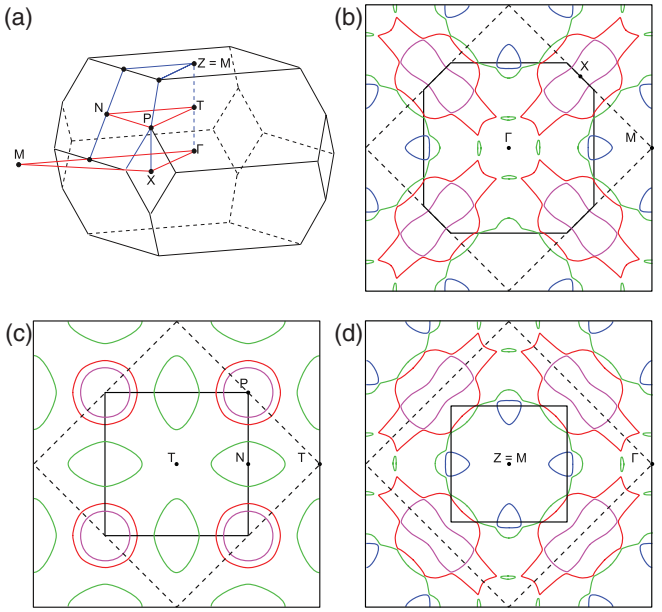

FIG. 3. (Color online) (a) Brillouin zone of $SrPd_2Ge_2$ and (b, c, d) cuts of the Fermi surface from the calculated electronic band structure for different k_z values.

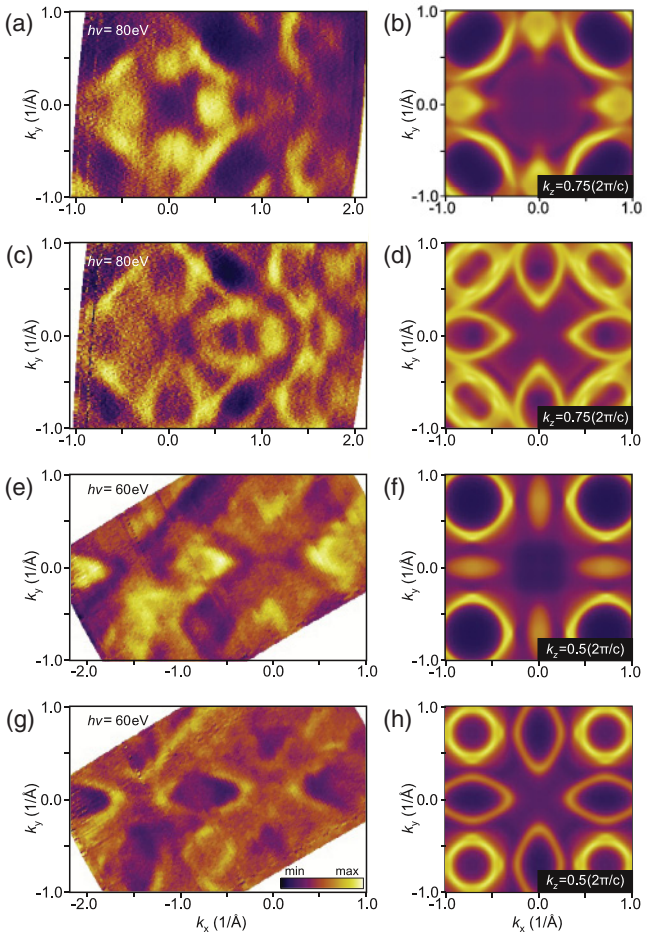

FIG. 4. (Color online) Comparison of the experimental and simulated MDMs: Photoemission intensity measured with (a) $h\nu = 80$ eV at the FL and (c) 500 meV below the FL and (b, d) the corresponding density of states calculated with $k_z = 0.75$ $(2\pi/c)$. Photoemission intensity measured with (e) $h\nu = 60$ eV at the FL and (g) 500 meV below the FL and (f, h) the corresponding density of states calculated with $k_z = 0.5$ $(2\pi/c)$. Sample temperature is 1.3 K.

$h\nu = 80$ and 60 eV at 1.3 K are shown in Fig. 4. Indeed, a very strong photon-energy dependence of the ARPES data is observed, indicating a strong k_z dependence of the Fermi surface.

In order to understand the experimentally observed FS topology, the two-dimensional MDMs with different k_z values have been simulated using the calculated electronic structure. By systematically varying k_z values, we found that the best agreement between experimental and calculated band structures is observed for $h\nu = 80$ eV and $k_z = 0.75$ $(2\pi/c)$, both for zero (FL) and 500-meV binding energies [see Figs. 4(a)–4(d)]. A binding-energy shift of 460 meV was applied to LDA band positions to match the k_F value of the Fermi-level crossing by the electron pocket around the X point. This shift of the LDA band structure is about 3 times bigger compared to pnictides and can be a result of the different orbital character of $SrPd_2Ge_2$ electronic bands. The same procedure gives the best agreement between the experimental and calculated band structures for $h\nu = 60$ eV and $k_z = 0.5$ $(2\pi/c)$ for both zero (FL) and 500-meV binding energies [see Figs. 4(e)–4(h)]. In both cases, the remarkable agreement between experimentally obtained and calculated band structures is observed.

Energy distribution maps (EDMs) for BZ cuts in high-symmetry directions for excitation photon energy $h\nu = 80$ eV are shown in Fig. 5. From the comparison of the experimental EDMs with the ones simulated using the calculated electronic band structure, we derive the band renormalization. For 122 iron pnictides LDA calculations usually give overestimated values for the band width compared to experimentally derived values from ARPES (Table I). But in the X-Γ-X EDM the separation between the bottoms of the two electron pockets around the X point is ~300 meV higher compared to LDA. Therefore one needs to apply a multiplier of 1.26 to LDA bands to get the best agreement with the experimentally derived band structure. This corresponds to the band renormalization factor of 0.8.

Another approach to obtain the value of renormalization of the band-forming electron pockets around the X point is to determine the Fermi velocity of the band at the Fermi level and compare it to the value from the calculated bare-band dispersion. Fitting the positions of momentum distribution curve maxima within first 200 meV below the Fermi level, we obtain the band dispersion and the corresponding value of the Fermi velocity. The ratio of calculated Fermi velocity $v_F^{LDA} = 4.45$ eV Å to experimental Fermi velocity $v_F^{ARPES} = 4.7$ eV Å gives the renormalization factor of $\sim 0.95 \pm 0.1$. This value is lower than in iron-based pnictide and chalcogenide superconductors, as presented in Table I. For example, for the isostructural compound KFe_2As_2 with a similar T_c of 3 K, the electron band-renormalization factor was reported to vary for different bands, from 2 to 4.[21]

This difference in the band renormalization can be explained by the different orbital characters of the Fermi surfaces of $SrPd_2Ge_2$ and of the iron pnictides. In the former, the corresponding bands are dominated by delocalized Ge p and Sr d states for which the effects of electronic correlations are treated well enough already by LDA. In the latter, on the other hand, the bands crossing the Fermi level are formed by moderately correlated Fe d states. The importance of the correlations seems to be confirmed by the dynamical mean-field-theory calculations, which give effective band-renormalization values of 2–3 for iron pnictides,[22–25] which are in a good agreement with ARPES data (Table I).

The weaker band mass renormalization, as compared with iron pnictides, together with the strong 3D character of the electronic structure and a nonmagnetic ground state suggest that superconductivity in $SrPd_2Ge_2$ is conventional and presumably of the electron-phonon nature. A recent study of the specific heat suggests a strong electron-phonon interaction in $SrPd_2Ge_2$;[8] however, it shows a significant deviation from the weak-coupling behavior in this material.

In order to clarify the nature of the superconductivity in $SrPd_2Ge_2$, one can use the knowledge of Fermi-surface topology, Fermi velocity, and energy gap and estimate values for the coherence length ξ and London penetration depth λ_L.[26] The Ginzburg-Landau parameter $\kappa = \lambda_L/\xi$ refers to the type of superconductor: type-I superconductors are those with $0 < \kappa < 1/\sqrt{2}$, and type-II superconductors are those with $\kappa > 1/\sqrt{2}$.

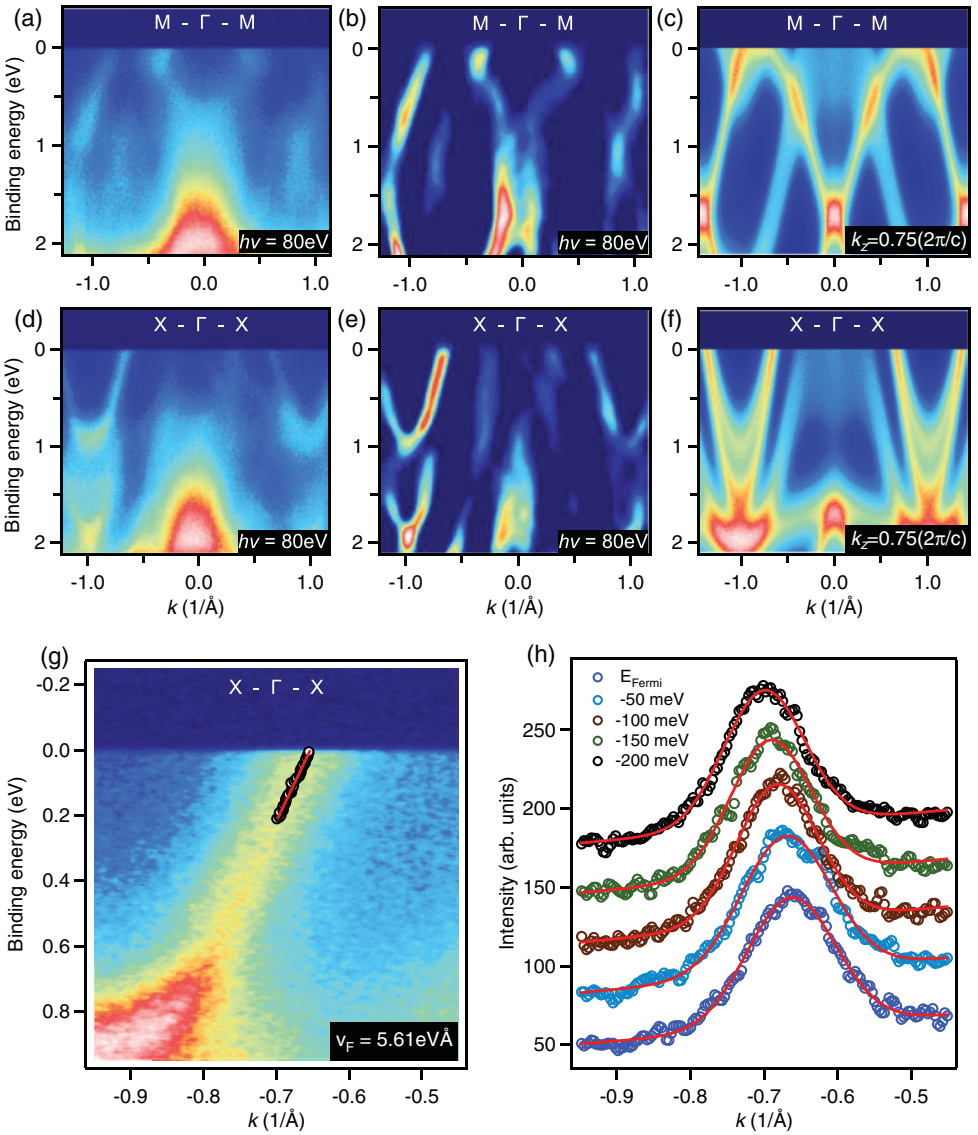

FIG. 5. (Color online) Comparison of the experimental and simulated energy distribution maps: Photoemission intensity measured with $h\nu = 80$ eV in the (a) M-Γ-M and (d) X-Γ-X directions, (b, 3) second derivatives, and (c, f) the corresponding density of states calculated with $k_z = 0.75\ (2\pi/c)$. (g) Photoemission intensity plot along the X-Γ-X direction together with extracted MDC peak positions (black circles) and linear fit (red line) to band dispersion; (h) the corresponding raw and fitted MDS. Sample temperature is 1.3 K.

The Cooper pair coherence length ξ and the magnetic field penetration depth λ_L can be estimated from microscopic parameters of the electronic spectrum as follows:[27,28]

$$\xi = \frac{\hbar v_F}{\pi \Delta} \propto \frac{v_F}{\Delta}, \tag{1}$$

$$\lambda_L = \left(\frac{e^2}{4\pi^2 \varepsilon_0 c^2 \hbar L_c} \int v_F dk \right)^{-\frac{1}{2}} \propto \frac{1}{\sqrt{\langle v_F \rangle \cdot \langle l_{\mathbf{k}}^{2D} \rangle}}, \tag{2}$$

where ε_0, $\hbar$, e, and c are physical constants, L_c is the c-axis lattice parameter, v_F is the Fermi velocity, $\langle l_{\mathbf{k}}^{2D} \rangle$ is the length of the Fermi contours (averaged over different k_z values for the three-dimensional case), and Δ is the value of the superconducting gap.

The superconducting energy gap of $SrPd_2Ge_2$ can be directly determined from low-temperature STS measurements.

TABLE I. Bandwidth renormalization factor m^*/m and superconducting transition temperature T_c for different iron pnictides.

Compound	m^*/m	T_c (K)	Reference
$BaFe_2As_2$	1.5		Ref. 14
$Ba_{0.6}K_{0.4}Fe_2As_2$	2.7	37	Ref. 14
$Ba_{0.6}K_{0.4}Fe_2As_2$	1.3–9	37	Ref. 15
$Ba(Fe_{0.94}Co_{0.06})_2As_2$	1.7	25	Ref. 14
LiFeAs	3	18	Ref. 16
$FeTe_{1-x}Se_x$	6–20	11.5	Ref. 17
$FeTe_{1-x}Se_x$	3	9	Ref. 18
NaFeAs	5.4–6.5	8	Ref. 19
LaFePO	2.2	5.9	Ref. 20
KFe_2As_2	2–4	3	Ref. 21
$SrPd_2Ge_2$	0.8–0.95	2.7	this work

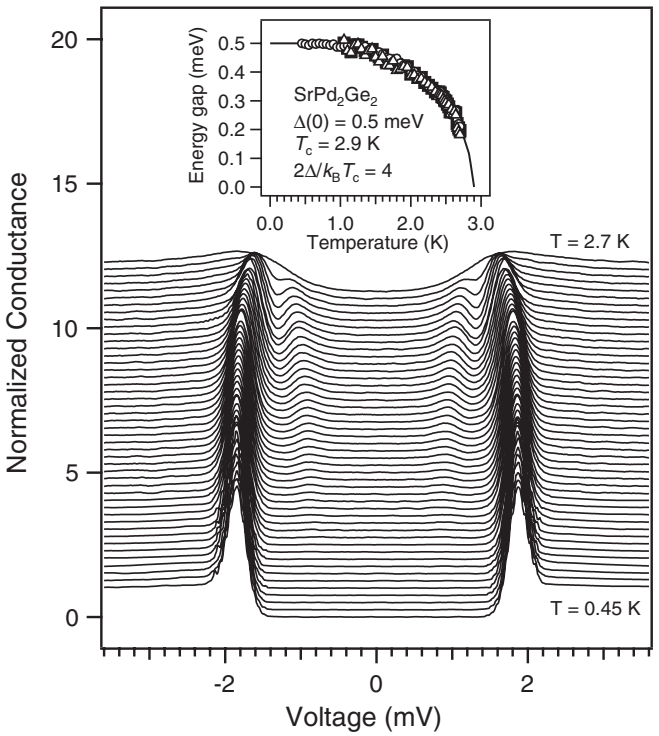

FIG. 6. STS conductance spectra of the superconductor-superconductor junction, Pb-$SrPd_2Ge_2$, measured in zero magnetic field at different temperatures between 0.45 K (lowest curve) and 2.7 K, increasing by 0.05 K (upper curves are shifted for clarity). The inset shows the temperature dependence of the superconducting gap of $SrPd_2Ge_2$ (circles, squares, and triangles) in comparison with the BCS theory (line).

Figure 6 shows the tunneling conductance spectra between the superconducting Pb tip and the $SrPd_2Ge_2$ sample measured at different temperatures ranging from 0.45 to 2.7 K. Each of these differential conductance versus voltage spectra is proportional to the convolution of the superconducting density of states of both electrodes forming a junction. All curves exhibit two large peaks located at approximately ± 1.86 mV for the lowest temperatures. These peaks, corresponding to the sum of the superconducting energy gaps of the tip and the sample, appear at voltages $\pm|\Delta_{Pb} + \Delta_S|/e$, where Δ_{Pb} and Δ_S are the superconducting energy gaps of the lead tip and the sample, respectively, and e is the electron's charge. In addition, at temperatures above 1.2 K, two minor peaks at approximately ± 0.86 mV come out. These peaks, corresponding to the difference of the superconducting energy gaps of the tip and the sample, appear at voltages $\pm|\Delta_{Pb} - \Delta_S|/e$ and represent the thermally activated current induced by excited quasiparticles above and corresponding holes below the superconducting energy gap of the sample. For the curves taken at the lowest temperatures the zero-conductance plateau in the center of the respective curve goes up to well above Δ_{Pb}. As temperature is raised, the dip appearing at approximately ± 1.3 mV between the two above-mentioned peaks reaches even negative conductance values. These two observations indicate that $SrPd_2Ge_2$ is indeed an s-wave single-gap superconductor, and $s^{\pm}$ pairing proposed for the isostructural 122 iron pnictides,[29] which has been associated with unconventional pairing mediated by magnetic fluctuations, is probably absent here.

The two pairs of peaks corresponding to $|\Delta_{Pb} + \Delta_S|$ and $|\Delta_{Pb} - \Delta_S|$ allow a direct determination of $\Delta_{Pb}(T)$ and $\Delta_S(T)$ from the tunneling curves. The superconducting energy-gap value of lead, $\Delta_{Pb} = 1.36$ meV, is obtained at the lowest temperature. It is in perfect agreement with the literature.[30] The superconducting energy-gap value of $SrPd_2Ge_2$, $\Delta_S(T)$, can then be estimated in three different fashions: first, by subtracting the values of the two peaks $(|\Delta_{Pb} + \Delta_S| - |\Delta_{Pb} - \Delta_S|)/2$, second, by subtracting Δ_{Pb} from $|\Delta_{Pb} + \Delta_S|$, and third, by subtracting $|\Delta_{Pb} - \Delta_S|$ from Δ_{Pb} (indicated by solid squares, open circles, and triangles in the inset of Fig. 6, respectively). All three estimates of $\Delta_S(T)$ coincide accurately with the prediction of the BCS theory. The resulting superconducting energy gap and critical temperature of $SrPd_2Ge_2$, measured by STS, are $\Delta(0) = 0.5$ meV and $T_c = 2.9$ K, indicating strong-coupling superconductivity with a ratio of $2\Delta/kT_c = 4.0$.

Taking the maximum value of the superconducting gap from STS data and the details of the Fermi-surface topology and Fermi velocity from ARPES data, in Table II, formulas (1) and (2) are used to estimate the in-plane Pippard superconducting coherence length and London penetration depth and, consequently, to evaluate the Ginzburg-Landau parameter. If for iron-pnictide superconductors in Table II the obtained Ginzburg-Landau parameter $\kappa \gg 1/\sqrt{2}$ indicates that these materials are type-II superconductors, then for $SrPd_2Ge_2$ the obtained $\kappa < 1/\sqrt{2}$ indeed points to a type-I superconductor, which contradicts magnetization measurements.[7,8]

This discrepancy in experimental results can be explained by taking into account the finite value of the electron mean free path l in a superconductor. If $l \ll \xi$, the superconductor is in a so-called "dirty limit," and the following corrections

TABLE II. Average Fermi velocity v_F, length of the Fermi contours $\langle l_{\mathbf{k}}^{2D} \rangle$, and the superconducting gap Δ_{max} for $(Ba,K)Fe_2As_2$, LiFeAs, $Ba(Fe,Co)_2As_2$, and $SrPd_2Ge_2$. The London penetration depth λ_L and the coherence length ξ are estimated from aforementioned parameters according to formulas (1) and (2). The Ginzburg-Landau parameter κ is shown in the last column.

Compound	$\langle v_F \rangle$ (eV Å)	$\langle l_{\mathbf{k}}^{2D} \rangle$ (Å^{-1})	Δ_{max} (meV)	λ_L (nm)	ξ (nm)	$\kappa = \lambda_L/\xi$
$(Ba,K)Fe_2As_2$	0.41[31]	$2\pi \times 0.74$[31]	10[32]	170	1.3	131
LiFeAs	0.31[16,26]	$2\pi \times 0.96$[16]	3[26]	172	3.3	52
$Ba(Fe,Co)_2As_2$	0.7[33]	$2\pi \times 0.61$	5	144	4.5	32
$SrPd_2Ge_2$	4.7	$\sim 2\pi \times 1.2$	0.5	40	299	0.13

TABLE III. The electron mean free path l, effective penetration depth λ^{eff}, and effective coherence length ξ^{eff} as calculated according to formulas (3) and (4). The effective Ginzburg-Landau parameter, $\kappa^{\text{eff}} = \lambda^{\text{eff}}/\xi^{\text{eff}}$, is shown in the last column.

Compound	ρ ($\mu\Omega$ cm)	l (nm)	λ^{eff} (nm)	ξ^{eff} (nm)	κ_{eff}
$(Ba,K)Fe_2As_2$	50[35]	4.5	193	1.3	149
LiFeAs	15[36]	11.4	195	2.9	67
$Ba(Fe,Co)_2As_2$	100[37,38]	2.8	233	2.8	83
$SrPd_2Ge_2$	70[8]	1.5	566	21.1	27

to the values for coherence length ξ and penetration depth λ apply:[34]

$$\xi^{\text{eff}} \approx \frac{\xi}{\sqrt{1+\xi/l}}, \quad \lambda^{\text{eff}} \approx \lambda_{\text{L}}\sqrt{1+\xi/l}. \tag{3}$$

The electrons mean free path l can be calculated using the following formula:[35,36]

$$l = \frac{1}{\rho}\frac{2\pi L_c h}{e^2\langle l_{\mathbf{k}}^{2\text{D}}\rangle}, \tag{4}$$

where ρ is resistivity value at $T = 0$, L_c is the size of the primitive elementary cell along the c axis, h is the Plank constant, e is the elementary charge, and $\langle l_{\mathbf{k}}^{2\text{D}}\rangle$ is the length of the Fermi contours (averaged over different k_z values for the three-dimensional case). In the case of $SrPd_2Ge_2$ the electron mean free path l calculated from conductivity data points to the superconductivity in a dirty limit, $l \ll \xi$ (in Table III). The corrected values for coherence length and penetration depth, $\xi^{\text{eff}} = 21.1$nm and $\lambda^{\text{eff}} = 566$ nm, are calculated using Eq. (3). These results are in a good agreement with the magnetization measurements, where the coherence length $\xi_{\text{GL}} = 21.34$ nm was obtained from the value of the upper critical field H_{c2} using the Ginzburg-Landau theory formula for coherence length $\xi_{\text{GL}} = \sqrt{\frac{\Phi_0}{2\pi H_{c2}}}$.[8] The corrected value for the Ginzburg-Landau parameter $\kappa^{\text{eff}} = 27$ shows that $SrPd_2Ge_2$ is a type-II superconductor in a dirty limit; also it is intrinsically a type-I superconductor, contrary to pnictides.

Therefore, the fact that $SrPd_2Ge_2$ is isostructural to the 122 family of iron pnictides does not necessarily lead to the same origin of the superconductivity. As has been recently suggested,[39] even iron pnictides within a single family may not necessarily share the same superconducting pairing mechanism. This is best demonstrated, for example, by the presence of unconventional superconductivity in $Ba(Fe_{1-x}Ni_x)_2As_2$ close to optimal doping ($x \approx 0.05$)[40,41] and the conventional phonon-mediated pairing in $BaNi_2As_2$ ($x = 1$).[42]

IV. SUMMARY

In conclusion, the occupied electronic structure of the pnictogen-free $SrPd_2Ge_2$ has been studied by means of ARPES and compared with first-principles calculations. At variance with isostructural iron-based superconductors, its electronic structure reveals a much more pronounced three-dimensional character. The 3D structure of the $SrPd_2Ge_2$ Fermi surface is confirmed by the remarkable agreement of LDA calculations with experimentally measured momentum distribution maps. In contrast to iron-based superconductors, the orbital composition of the conductance band is not dominated by the transition-metal d states, which are localized much deeper below the Fermi level, but represents a mixture of Sr d, Pd d, and Ge p states.

By comparing the experimental and calculated band structures, the values of the out-of-plane component of the electron momentum corresponding to the photoemission spectra obtained with different excitation photon energies has been determined.

Using the ratio of the calculated bare Fermi velocity to the experimental one, the band renormalization factor of ~0.95 has been obtained. This relatively small value of electron band renormalization together with a relatively low T_c as compared to iron pnictides and chalcogenides support the conventional phonon-mediated mechanism of superconductivity in this pnictogen-free compound.

The STS measurements show that $SrPd_2Ge_2$ is a strong-coupling single s-wave gap superconductor, with superconducting energy gap $\Delta(0) = 0.5$ meV and the BCS-like temperature dependence of the gap.

The estimation for the Ginzburg-Landau parameter $\kappa = 0.14$ obtained from ARPES and STS data indicates that $SrPd_2Ge_2$ is likely to be a type-I superconductor. But additional calculations of the electron mean free path from conductivity data show that $SrPd_2Ge_2$ is a type-II superconductor in the dirty limit with $\kappa^{\text{eff}} = 27$, in agreement with the conclusions from magnetization studies.[7,8] Preliminary STM investigations reveal the presence of a superconducting vortex structure, indicating a type-II superconductivity in the dirty limit, which is in accordance with our results and the magnetization measurements.[43]

ACKNOWLEDGMENTS

This work was supported by the DFG priority program SPP1458, Grants No. KN393/4, BO1912/2-1, and No. BO3537/1-1 (D.S.I. and J.T.P.); by the Slovak Research and Development Agency under Contract No. VVCE-0058-07, Slovak VEGA Grants No. 0148/10 and No. 1/0138/10, and the 7th FP MNT-ERA.Net II. ESO (T.S., P.S., J.G.R, and P.S.); by the Spanish MEC under projects Consolider Ingenio Molecular Nanoscience CSD2007-00010 and FIS2008-00454 (J.G.R.); and by the Korean government (MEST) Grants No. R15-2008-006-01002-0 and 2011-0028736 (N.H.S., B.K.C.).

*timur.kim@diamond.ac.uk

[1] Y. Kamihara, T. Watanabe, M. Hirano, and H. Hosono, J. Am. Chem. Soc. **130**, 3296 (2008).

[2] K. Ishida, Y. Nakai, and H. Hosono, J. Phys. Soc. Jpn. **78**, 062001 (2009).

[3] J. Paglione and R. L. Green, Nat. Phys. **6**, 645 (2010).

[4]Z. Ren, Q. Tao, S. Jiang, C. Feng, C. Wang, J. Dai, G. Cao, and Z. Xu, Phys. Rev. Lett. **102**, 137002 (2009).

[5]S. Jiang, H. Xing, G. Xuan, C. Wang, Z. Ren, C. Feng, J. Dai, Z. Xu, and G. Cao, J. Phys. Condens. Matter **21**, 382203 (2009).

[6]J. Orenstein and A. J. Millis, Science **288**, 468 (2000); C. C. Tsuei and J. R. Kirtley, Rev. Mod. Phys. **72**, 969 (2000).

[7]H. Fujii and A. Sato, Phys. Rev. B **79**, 224522 (2009).

[8]N. H. Sung, J. S. Rhyee, and B. K. Cho, Phys. Rev. B **83**, 094511 (2011)

[9]J. G. Rodrigo, H. Suderow, S. Vieira, E. Bascones, and F. Guinea, J. Phys. Condens. Matter **16**, R1151 (2004).

[10]S. V. Borisenko *et al.* (unpublished).

[11]O. Krogh Andersen, Phys. Rev. B **12**, 3060 (1975).

[12]A. Y. Perlov, A. N. Yaresko, and V. N. Antonov, PYLMTO, a spin-polarized relativistic linear muffin-tin orbitals package for electronic structure calculations (unpublished).

[13]I. R. Shein and A. L. Ivanovskii, Phys. B **405**, 3213 (2010).

[14]M. Yi, D. H. Lu, J. G. Analytis, J.-H. Chu, S.-K. Mo, R.-H. He, R. G. Moore, X. J. Zhou, G. F. Chen, J. L. Luo, N. L. Wang, Z. Hussain, D. J. Singh, I. R. Fisher, and Z.-X. Shen, Phys. Rev. B **80**, 024515 (2009).

[15]H. Ding, K. Nakayama, P. Richard, S. Souma, T. Sato, T. Takahashi, M. Neupane, Y.-M. Xu, Z.-H. Pan, A. V. Fedorov, Z. Wang, X. Dai, Z. Fang, G. F. Chen, J. L. Luo, and N. L. Wang, J. Phys. Condens. Matter **23**, 135701 (2011).

[16]S. V. Borisenko, V. B. Zabolotnyy, D. V. Evtushinsky, T. K. Kim, I. V. Morozov, A. N. Yaresko, A. A. Kordyuk, G. Behr, A. Vasiliev, R. Follath, and B. Büchner, Phys. Rev. Lett. **105**, 067002 (2010).

[17]A. Tamai, A. Y. Ganin, E. Rozbicki, J. Bacsa, W. Meevasana, P. D. C. King, M. Caffio, R. Schaub, S. Margadonna, K. Prassides, M. J. Rosseinsky, and F. Baumberger, Phys. Rev. Lett. **104**, 097002 (2010).

[18]F. Chen, B. Zhou, Y. Zhang, J. Wei, H.-W. Ou, J.-F. Zhao, C. He, Q.-Q. Ge, M. Arita, K. Shimada, H. Namatame, M. Taniguchi, Z.-Y. Lu, J. Hu, X.-Y. Cui, and D. L. Feng, Phys. Rev. B **81**, 014526 (2010).

[19]C. He, Y. Zhang, B. P. Xie, X. F. Wang, L. X. Yang, B. Zhou, F. Chen, M. Arita, K. Shimada, H. Namatame, M. Taniguchi, X. H. Chen, J. P. Hu, and D. L. Feng, Phys. Rev. Lett. **105**, 117002 (2010).

[20]D. H. Lu, M. Yi, S.-K. Mo, A. S. Erickson, J. Analytis, J.-H. Chu, D. J. Singh, Z. Hussain, T. H. Geballe, I. R. Fisher, and Z.-X. Shen, Nature (London) **455**, 81 (2008).

[21]T. Sato, K. Nakayama, Y. Sekiba, P. Richard, Y.-M. Xu, S. Souma, T. Takahashi, G. F. Chen, J. L. Luo, N. L. Wang, and H. Ding, Phys. Rev. Lett. **103**, 047002 (2009).

[22]S. L. Skornyakov, A. V. Efremov, N. A. Skorikov, M. A. Korotin, Yu. A. Izyumov, V. I. Anisimov, A. V. Kozhevnikov, and D. Vollhardt, Phys. Rev. B **80**, 092501 (2009).

[23]A. Kutepov, K. Haule, S. Y. Savrasov, and G. Kotliar, Phys. Rev. B **82**, 045105 (2010).

[24]K. Haule, J. H. Shim, and G. Kotliar, Phys. Rev. Lett. **100**, 226402 (2008).

[25]M. S. Laad, L. Craco, S. Leoni, and H. Rosner, Phys. Rev. B **79**, 024515 (2009).

[26]D. S. Inosov, J. S. White, D. V. Evtushinsky, I. V. Morozov, A. Cameron, U. Stockert, V. B. Zabolotnyy, T. K. Kim, A. A. Kordyuk, S. V. Borisenko, E. M. Forgan, R. Klingeler, J. T. Park, S. Wurmehl, A. N. Vasiliev, G. Behr, C. D. Dewhurst, and V. Hinkov, Phys. Rev. Lett. **104**, 187001 (2010).

[27]M. Tinkham, *Introduction to Superconductivity* (McGraw-Hill, New York, 1975).

[28]B. S. Chandrasekhar and D. Einzel, Ann. Phys. (Leipzig) **505**, 535 (1993).

[29]M. L. Teague, G. K. Drayna, G. P. Lockhart, P. Cheng, B. Shen, H.-H. Wen, and N.-C. Yeh, Phys. Rev. Lett. **106**, 087004 (2011).

[30]Ch. Kittel, *Introduction to Solid State Physics* (Wiley, New York, 1996).

[31]D. V. Evtushinsky, D. S. Inosov, V. B. Zabolotnyy, M. S. Viazovska, R. Khasanov, A. Amato, H.-H. Klauss, H. Luetkens, Ch. Niedermayer, G. L. Sun, V. Hinkov, C. T. Lin, A. Varykhalov, A. Koitzsch, M. Knupfer, B. Büchner, A. A. Kordyuk, and S. V. Borisenko, New J. Phys. **11**, 055069 (2009).

[32]D. V. Evtushinsky, D. S. Inosov, V. B. Zabolotnyy, A. Koitzsch, M. Knupfer, B. Büchner, M. S. Viazovska, G. L. Sun, V. Hinkov, A. V. Boris, C. T. Lin, B. Keimer, A. Varykhalov, A. A. Kordyuk, and S. V. Borisenko, Phys. Rev. B **79**, 054517 (2009).

[33]The extraction of the electronic band parameters for Co-doped 122 iron arsenide $Ba(Fe, Co)_2As_2$ from ARPES data will be presented elsewhere.

[34]From the Ginzburg-Landau theory the following exact formulas for the effective coherence length ξ and penetration depth λ can be obtained: $\xi^{\text{eff}} = \frac{\pi}{2\sqrt{3}} \frac{\xi}{\sqrt{1+t\xi/l}}$ and $\lambda^{\text{eff}} = \lambda_{\text{L}}\sqrt{1+t\xi/l}$, where t is a constant equal to 1 for $T = 0$ and 3/4 for $T = T_c$.[27]

[35]D. V. Evtushinsky, A. A. Kordyuk, V. B. Zabolotnyy, D. S. Inosov, T. K. Kim, B. Büchner, H. Luo, Z. Wang, H.-H. Wen, G. Sun, C. Lin, and S. V. Borisenko, J. Phys. Soc. Jpn. **80**, 023710 (2011).

[36]O. Heyer, T. Lorenz, V. B. Zabolotnyy, D. V. Evtushinsky, S. V. Borisenko, I. Morozov, L. Harnagea, S. Wurmehl, C. Hess, and B. Büchner, Phys. Rev. B **84**, 064512 (2011).

[37]L. Fang, H. Luo, P. Cheng, Z. Wang, Y. Jia, G. Mu, B. Shen, I. I. Mazin, L. Shan, C. Ren, and H.-H. Wen, Phys. Rev. B **80**, 140508(R) (2009).

[38]Y. J. Yan, X. F. Wang, R. H. Liu, H. Chen, Y. L. Xie, J. J. Ying, and X. H. Chen, Phys. Rev. B **81**, 235107 (2010).

[39]D. S. Inosov, J. T. Park, A. Charnukha, Y. Li, A. V. Boris, B. Keimer, and V. Hinkov, Phys. Rev. B **83**, 214520 (2011).

[40]L. J. Li, Y. K. Luo, Q. B. Wang, H. Chen, Z. Ren, Q. Tao, Y. K. Li, X. Lin, M. He, Z. W. Zhu, G. H. Cao, and Z. A. Xu, New J. Phys. **11**, 025008 (2009).

[41]S. Chi, A. Schneidewind, J. Zhao, L. W. Harriger, L. Li, Y. Luo, G. Cao, Z. Xu, M. Loewenhaupt, J. Hu, and P. Dai, Phys. Rev. Lett. **102**, 107006 (2009).

[42]N. Kurita, F. Ronning, C. F. Miclea, Y. Tokiwa, E. D. Bauer, A. Subedi, D. J. Singh, H. Sakai, J. D. Thompson, and R. Movshovich, J. Phys. Conf. Ser. **273**, 012097 (2011).

[43]T. Samuely *et al.* (unpublished).